# Interaction of #-Thymidine Inhibitors with Thymidylate Kinase from Plasmodium falciparum

Mengshen Chen, Kaustubh Sinha, Gordon S. Rule, and Danith H. Ly

*Biochemistry*, **Just Accepted Manuscript** • DOI: 10.1021/acs.biochem.8b00162 • Publication Date (Web): 23 Apr 2018

Interaction of α-Thymidine Inhibitors with Thymidylate Kinase from *Plasmodium falciparum*.

Mengshen (David) Chen[a], Kaustubh Sinha[a], Gordon S. Rule[a], Danith H. Ly[b*]

[a] Department of Biological Sciences, Carnegie Mellon University, 4400 5th Ave, Pittsburgh PA.

[b] Department of Chemistry, Carnegie Mellon University, 4400 5th Ave, Pittsburgh PA.

[*] Corresponding author, dly@andrew.cmu.edu. Tel: (412) 268-4010.

**Abstract**

*Plasmodium falciparum* thymidylate kinase (PfTMK) is a critical enzyme in the de novo biosynthesis pathway of pyrimidine nucleotides. N-(5'-deoxy-α-thymidin-5'-yl)-N'-(4-(2-chlorobenzyloxy)phenyl)urea was developed as an inhibitor of PfTMK and has been reported as an effective inhibitor of *P. falciparum* growth with an $EC_{50}$ of 28 nM (Cui et al, (2012) Journal of Medicinal Chemistry, 55, 10948-10957). Using this compound as a scaffold, a number of derivatives were developed, and, along with the original compound, were characterized in terms of their enzyme inhibition ($K_i$) and binding affinity ($K_D$). Furthermore, the binding site of the synthesized compounds was investigated by a combination of mutagenesis and docking simulations. Although the reported compound is indicated to be highly effective in its inhibition of parasite growth, we observed significantly weaker binding affinity and inhibition of PfTMK than expected from the reported $EC_{50}$. This suggests that significant structural optimization will be required for the use of this scaffold as an effective PfTMK inhibitor and that the inhibition of parasite growth is due to an off-target effect.

## Introduction

Malaria is one of the most devastating parasite-borne infectious diseases with over 200 million infections and over 500,000 deaths each year. *Plasmodium falciparum*, the deadliest form of malaria parasite, is responsible for the mortality and morbidity of malaria infection. Current treatments against *P. falciparum* malaria include Artemisinin Combination Therapies (ACTs). Although ACTs work quite well against malaria, there is widespread resistance to many anti-malarial drugs. The resistance has arisen due to counterfeit or substandard treatments, unregulated administration of drugs, and the lack of complementary combination treatment, such as lumefantrine[1]. Due to increased drug resistance there is a continuing need to develop additional anti-malarial compounds.

The development of malaria infection is divided into two phases: exoerythrocytic phase and erythrocytic phase[2], both of which require large amounts of deoxythymidine-5'-triphosphate (dTTP) for DNA replication. *P. falciparum* lacks the ability to salvage pyrimidines[3], consequently it relies solely on *de novo* pyrimidine nucleoside synthesis to support the high dTTP demand during rapid DNA replication in the erythrocytic phase. One of the enzymes in the biosynthetic pathway to dTTP is thymidylate kinase (TMK). Thymidylate kinases are unique in that they are the only nucleotide kinase that facilitates the phosphorylation of deoxythymidine-5'-monophosphate (dTMP) to deoxythymidine-5'-diphosphate (dTDP).

X-ray crystal structures of ligand-bound TMKs have been solved in various organisms, such as human[4],*Saccharomyces cerevisiae*[5], *Mycobacterium tuberculosis*[6], *Vaccinia virus*[7], *P. falciparum*[8], and *Candida albicans*[9]. All TMKs are homodimers, each subunit consists of five stranded parallel β–sheets and 7 to 11 α–helices. There are two conserved motifs in the nucleotide binding domain: a P-loop, which is involved with substrate recognition and enzyme catalysis, and a LID domain, which plays a part in catalysis[10].

The low sequence similarity between huTMK and TMKs from bacteria and fungi suggests that inhibitors of non-human TMKs are potential antibiotics because they would selectively interfere with DNA replication in the pathogen without inhibition of huTMK. Correspondingly, a number of groups have developed inhibitors of TMKs from a variety of pathogens, including gram positive bacteria[11, 12], *Mycobacterium tuberculosis*[13, 14], and *Pseudomonas aeruginosa*[15].

The superposition of the enzyme-substrate complex for human TMK (huTMK) and PfTMK

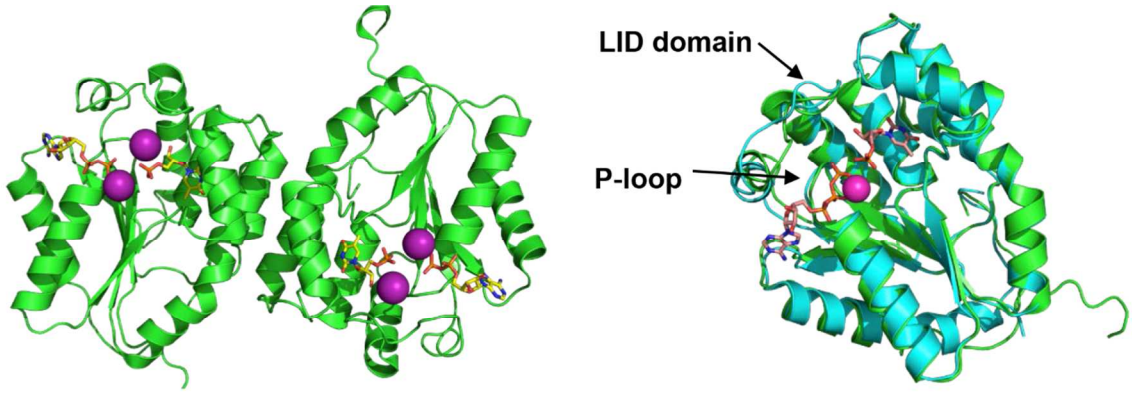


**Figure 1. X-ray crystal structure of PfTMK.** Left Panel: PfTMK dimer complexed with ADP, dTMP, and Na+ (pdb 2WWF). Right Panel: Overlay of huTMK (green) and PfTMK (cyan). X-ray crystal structure of huTMK (pdb 1NN0) is superimposable on that of PfTMK (pdb 2WWF), except for the LID domain. Purple spheres represent bound $Mg^{+2}$ ions.

suggests that the human and Plasmodium enzymes are highly similar in their topology (see Figure 1). However, the low sequence similarity (40%) between huTMK and PfTMK (see Figure 2), and the fact that PfTMK is one of the few TMKs that can also phosphorylate dGMP, indicates that it should be feasible to develop effective anti-malarial drugs that are specific inhibitors of PfTMK[3]. Kato *et al*[16] explored racemic carbocyclic derivatives of thymidine and obtained $K_I$ values for PfTMK which were as low as 20 μM for compound A (Chart 1). Noguchi *et al*[17] subsequently prepared pure enantiomers of derivative of compound A, producing compounds

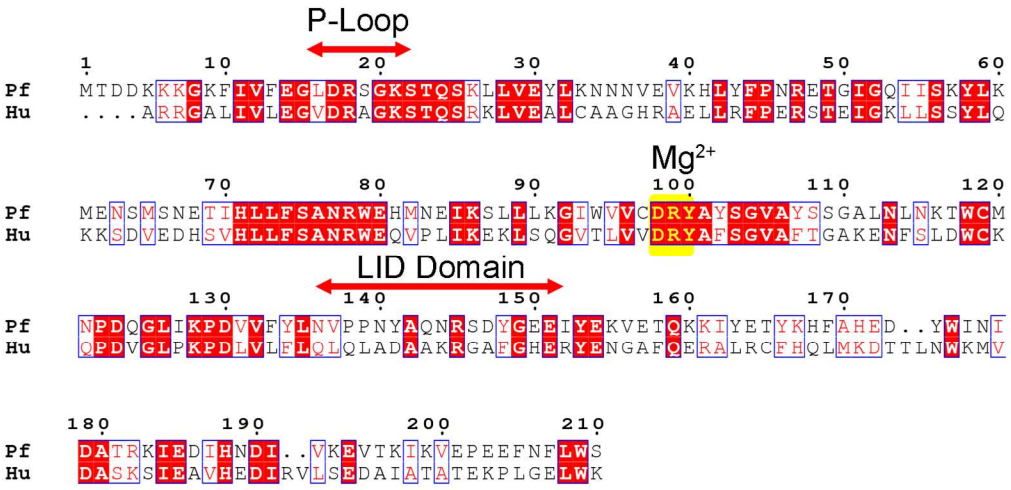


**Figure 2. Sequence alignment of PfTMK and HuTMK..** The P-loop motif is well conserved between PfTMK (top, Pf) and HuTMK (lower, Hu), but not the LID domain, which explains the superimposable P-loop and non-superimposable LID domain in the overlay structure. The conserved $Mg^{+2}$ binding site is labeled and highlighted.

with slightly higher affinity. Cui *et al* reported the development of a large number of inhibitors of PfTMK[8]. These compounds were based on an α-thymidine thiourea inhibitor of TMK from *Mycobacterium tuberculosis*. They established that α-thymine inhibitors are more potent than β-thymidine, and that replacement of the thiourea with urea improved inhibition. Cui reported that N-(5'-deoxy-α-thymidin-5'-yl)-N'-(4-(2-chlorobenzyloxy)phenyl)urea (compound B, chart 1) was the most effective inhibitor of *P. falciparum* growth, with an EC50 value of 28 nM and a $CC_{50}$ of 29 μM. However, the ability of compound B to inhibit PfTMK was not reported, consequently it is

not possible to determine whether its effectiveness is due to inhibition of PfTMK, or some other target in the organism.

Although an effective inhibitor of growth, compound B is metabolically unstable, likely due to the presence of the chlorobenzene substituent. In the liver, chlorobenzene quickly goes through oxidation to form an epoxide, and the epoxide is either hydrolyzed or conjugated to glutathione to form pre-mercapturic acid[18].

Here, we report the synthesis of a number of derivatives of compound B (see scheme 1). We have fully characterized the original compound and two of these derivatives, where the chlorine was replaced by with fluorine or a methoxy group. These compounds were characterized to test whether the chlorobenzene group is unique in conferring compound B the ability to potentially inhibit PfTMK. We also wanted to explore the effect of replacing the chlorine atom with metabolically more stable fluorine[19] on the interaction with PfTMK. We have quantified the binding of these inhibitors to PfTMK ($K_D$) and measured their ability to inhibit PfTMK and report $K_i$ values. Although the Cl-derivative has a low $EC_{50}$ value (28 nM), the experimentally measured $K_i$ and $K_D$ values reported here are significantly higher (200 μM), and unaffected by the substitution of chlorine with fluorine or methoxy. Docking simulations show that these compounds bind to the same region of the active site as dTMP and the benzyloxy-phenyl group

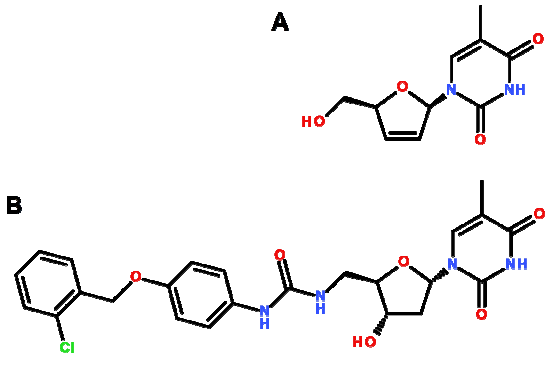


Chart 1: Inhibitors of PfTMK. The chlorobenzene group in B was replaced by H, F, $CH_3$ and -O-$CH_3$ in this work.

approaches the binding site for ATP. We verified the binding site of these compounds to PfTMK by generating a mutant PfTMK and show that this mutation greatly reduces the binding affinity. Our data suggest that compound B will require significant modification to increase its effectiveness as a PfTMK inhibitor and that the intracellular target of this compound is unlikely to be PfTMK and the inhibition of parasite growth is likely due to an off-target effect.

## Materials and Methods

Synthesis of prospective inhibitors:

The general synthetic approach is outlined in Scheme 1 and additional details are provided in the supporting information. The 5' hydroxyl group of β-thymidine is protected with diphenylacetyl group (compound 10), this was followed by protection of the 3' hydroxyl group with a p-toluoyl group (compound 11). These two specific protecting groups were chosen because they are beneficial for the crystallization of C1'-epimerization product[20]. Racemization was then carried out to convert β-anomer to α-anomer (compound 12)[21, 22]. After the racemization, the protecting groups were removed (compound 13), this was followed by a 3-step amination of 5' hydroxyl (selective sulfonylation of 5' hydroxyl, azidation of sulfonyl group, and hydrogenation) to yield the amine compound 16. Meanwhile, various benzyl bromide derivatives (5a-d) were coupled to Boc-protected 4-aminophenol (compound 6a-6d), this was followed by the removal of the Boc protecting group (compound 7a-7d), and synthesis of isocyanate derivatives using triphosgene

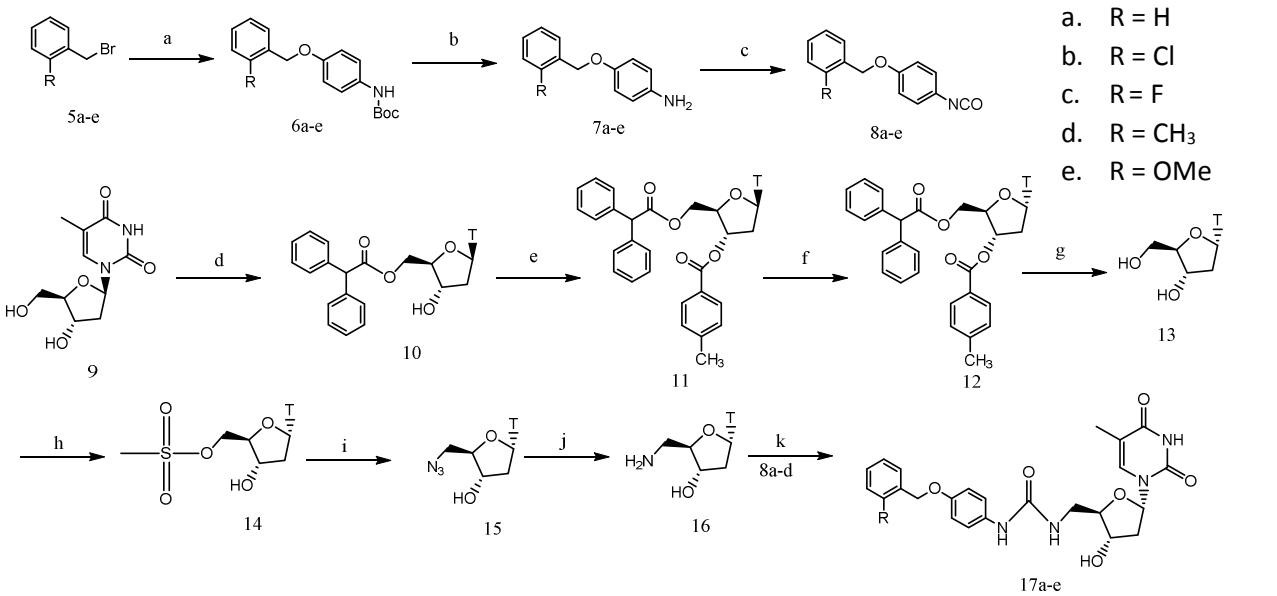


**Scheme 1. Library synthesis**. *Reagents and conditions*: (a) NaH, N-Boc protected 4-aminophenol, DMF, 0°C, 1.5 hrs; (b) TMS-Cl, MeOH, RT, 3 hrs; (c) Et3N, triphosgene, EtOAc, 77°C, 3 hrs; (d) Diphenylacetyl chloride, pyridine, DCM, 0°C, overnight; (e) p-toluoyl chloride, pyridine, DCM, RT, overnight; (f) Acetic anhydride, $H_2SO4$, ACN, RT, 3 hrs; (g) NaOMe, MeOH, RT, 3 hrs; (h) MsCl, pyridine, -38°C, 1 hr, 0°C, 3hrs; (i) $NaN_3$, DMF, RT, 3 hrs; (j) 10% Pd/C, MeOH, RT, 3 hrs; (k) DMF, RT, 3 hrs.

(compound 8a-8d). Lastly, the two halves were coupled together to yield final compounds (17a-17d).

Synthesis of the methoxy derivative (17e) did not fully follow this general synthetic scheme as the starting materials for this derivative was not commercially available. Instead, 3-methoxybenzyl alcohol was reacted with phosphotribromide in dichloromethane (DCM) for 3 hours at 0 ºC to generate compound 5e, and the rest of the synthesis procedure to the final compound 17e followed the general synthetic scheme.

Our synthesis procedures generally followed that of Cui *et al*[8]. However, some of the published synthetic strategies had unacceptably low yields. Consequently, conditions and reagent optimizations were made for the synthesis of the prospective inhibitors: the removal of Boc-protecting group from compounds 6a – e were carried out by dissolving the starting materials in methanol, then slowly titrating in one equivalence of trimethylsilane chloride, the reaction was carried out at room temperature for two hours, giving the following yields: 6a (96%), 6b (92%), 6c (92%), 6d (86%), and 6e (96%).

Additional changes in the synthesis including increasing the reaction time for the 3'- and 5'-protection of β-thymidine to overnight for optimal yield; and the azidation reaction of compound 14 was performed at 100°C overnight, the reaction mixture was then subjected to high-vacuum for solvent removal, and was re-dissolved in ethanol, the precipitate was then removed, and the ethanol filtrate was concentrated and subjected to column chromatography to purify compound 15.

Protein expression and purification:

A DNA sequence for PfTMK that was optimized for expression in *Escherichia coli* was obtained from DNA 2.0, with a $(His)_6$ tag at the amino terminus for the purification purpose. This DNA was cloned into the T7 expression plasmid pET-22b[23] and used to transform C3013 cells (New

England Biolabs). Clones that expressed PfTMK were maintained with 50 mg/ml of ampicillin. For the production of non-isotopically labelled protein, a single colony was inoculated into 5ml of Luria Broth (LB), grown overnight, transferred to larger volume of LB media, and induced for 3 hours with 1mM isopropylthiogalactoside (IPTG) after the optical density (OD600) at 600 nm reached 0.7.

Isotopically labeled PfTMK was produced by inoculating a colony into 1 ml of Studier's PG media[24] with 50% $H_2O$ and 50% $D_2O$ for overnight growth. The $D_2O$ level was increased by adding additional 4ml of the $D_2O$ media the next day and incubated for 5 hours. The cells were then harvested and transferred to a larger volume of PG media containing 100% $D_2O$. Once the OD600 reached 1.4, precursors were added to the culture (ketobutyric acid – methyl $^{13}C$ (50 mg/L) and alpha – ketoisovaleric acid (100 mg/L)[25]). The culture was then incubated at 30°C for 1 hour, and then induced with 1mM IPTG for 18 hours.

The induced cells were harvested and resuspended in 20 ml of lysis buffer (50 mM potassium phosphate, 250 mM NaCl, 5 mM imidazole, 0.02% azide, 10% glycerol, 0.1 mM ADP, 0.1 mM TMP, 10 mM MgSO4, pH 7.4) followed by the addition of lysozyme (1mg/ml) followed by incubation for 30 min at room temperature. This was followed by the addition of 1% Triton-X and sonication with Fisher Scientific 550 Sonicator. The lysate was subjected to centrifugation (19,000 g for 30 minutes) and the supernatant was collected and incubated with 5ml Hispur cobalt resin (Thermal Scientific) for 1 hour at 4 ºC. The supernatant-resin mixture was loaded onto a gravity column and was washed with 10-column volumes of wash buffer (50 mM potassium phosphate, 250 mM NaCl, 5 mM imidazole, 0.02% azide, pH 7.4). Lastly, the protein was eluted with 6-column volumes of elution buffer (50 mM sodium phosphate, 300 mM NaCl, 450 mM imidazole, pH 7.4). Buffer exchange was performed with Amicon Ultra concentrator to remove the high concentration of imidazole in the protein sample. The protein sample was then loaded on to a Q-Sepharose column that was pre-equilibrated with column buffer (20 mM

potassium phosphate, 0.92% sodium azide, 1 mM EDTA, pH 8.0). The protein was then eluted with a linear salt gradient from 0M to 2 M NaCl in column buffer, and the eluate was collected on fraction collector. The purified protein was then concentrated and stored at 4 ºC, typical yields are 50 mg of PfTMK from 1 L of culture.

*NADH Coupled Assay*

The NADH coupled assay[26] was performed to measure the $K_M$ of PfTMK for TMP, and to estimate the $K_i$ of the Cl-, F-, and OMe-derivatives (17b, 17c, 17e) against PfTMK.

In the measurement of $K_M$ of PfTMK for TMP, 1 ml kinase reactions contained 50 mM Tris-HCl, 50 mM KCl, 0.5 mM phosphoenolpyruvate, 1 mM ATP, 20 mM $Mg^{2+}$, 5 U/ml lactate dehydrogenase, 5 U/ml pyruvate kinase, 0.15 mM NADH, and a range of concentrations of TMP from 2 to 150 μM. The reaction was initiated by the addition of 200 nM of PfTMK and the absorbance at 340 nm was measured as a function of time.

The $K_i$ values for Cl-, F-, and OMe-derivatives were obtained by adding the compound to the reaction mixture prior to the addition of enzyme. We determined the initial velocities at various TMP concentrations (2 to 150 μM) in the presence of saturated ATP concentrations, and in the presence of various concentrations (100, 200, and 300 μM) of each compound. The $K_i$ for each compound were obtained using a Dixon plot.

*Tryptophan fluorescence and titration assay*

Tryptophan fluorescence titration experiments were conducted to determine the binding affinity of the Cl-, F-, and OMe-derivatives to PfTMK. The general experimental conditions were 300 nM PfTMK and 20 mM $Mg^{2+}$ in Tris buffer pH 7.4. 50 μl of the reaction mixture was pipetted into the wells on a 384-well plate. The Tryptophan fluorescence was measured with Tecan Infinite M1000 plate reader with excitation at 280nm and recording the fluorescence intensity as a function of wavelength (288 to 500 nm) for 80, 120, 160, 200, 240, 280, 320, 360, and 400 μM

of each compound. The $K_D$ for each of the synthesized compound was estimated by fitting the experimental values of ΔF to the following equation: $\Delta F = \Delta F_{max}[C]/(K_D+[C])$ using the Solver routine in Excel.

*Generation of F74A mutant*

Site-directed mutagenesis was performed to generate F74A mutant PfTMK using standard PCR methods[27]. The presence of the mutation was verified by Sanger sequencing of the entire coding region and the protein preparation and purification followed the same procedure as described above. The structural integrity of the F74A mutant was assessed by comparison of a two-dimensional HMQC methyl carbon spectra for the mutant and wild-type enzymes. The kinetic activity of the mutant protein was examined using the NADH-coupled assay. The activity of the F74A mutant was evaluated through NADH-coupled assay and no enzymatic activity was detected, consistent with the previous findings by Kandeel et al[28]. The binding properties to the F74A protein were examined by tryptophan fluorescence titration assay.

*Docking simulation*

The docking simulation experiments were carried out using Autodock Vina[29]. In our docking simulations, we used the X-ray crystal structure of PfTMK in complex with TMP (pdbid 2WWF)[10]. The 3D structure of the ligands were prepared with Chemsketch version 14.01[30] and the PDBQT format of both the receptor and ligands were prepared with Autodock Tools[31]. All water and solvent atoms were removed, and the polar hydrogens were added prior to docking simulation. The grid box was generated centering the TMP binding site of PfTMK and the coordinates of the grid box were then fed to Autodock Vina for the docking simulation calculations. Molecular structure images were prepared using Pymol, version 1.8[32].

## Results and Discussion

Our synthetic procedure generally followed previous literature methods[8, 21, 33] with modifications as described above. One of the most crucial steps in this procedure is the racemization of 3' and 5' protected β-thymidine to its α-thymidine anomer. The reaction was closely followed by thin-layer chromatography (TLC), the reactant and the product exhibit distinguishable $R_f$ values, and the reaction was terminated after the reactant was fully consumed. The identities of compounds 11 and 12 were determined by proton NMR. The end products: compounds 17a to 17e were confirmed by both proton NMR and mass-spec (Supporting information Figure S1 to S5). The Cl-derivative (17b) was further evaluated through a series of 2D NMR experiments, including HMBC, HSQC, and COSY (not shown).

Compounds 17b, 17c, and 17e were utilized in subsequent kinetics and binding assay. Although compound 17b was previously characterized *in vivo*[8], its *in vitro* $K_D$ and $K_i$ values were not reported. Compounds 17c and 17e were characterized because 17b contains a pharmacologically unstable chloro-benzene substituent while 17c and 17e are substituted with electron-withdrawing and electron-donating groups, i.e. fluoro-benzene, and methoxy-benzene.

PfTMK Inhibition:

NADH-coupled assay was performed to experimentally measure the $K_M$ and $k_{cat}$ of PfTMK for TMP, and to examine the inhibition effect of compounds 17b, c, and e. The $K_{cat}$ of WT PfTMK was measured to be 3.14±0.10 $s^{-1}$, and the $K_M$ for TMP for PfTMK was 25.5±0.49 μM (triplicate measurements); our experimental values for both the $k_{cat}$ and $K_M$ are consistent with previously published data[28, 34].

| Compound | $K_D$ (μM) | $K_i$ (μM) |
|---|---|---|
| Cl-derivative (17b) | 175 ± 2 | 225 |
| F-derivative (17c) | 177 ± 15 | 205 |
| OMe-derivative (17e) | 181 ± 1 | 220 |

***Table 1***. $K_D$ and $K_I$ values for compounds 17b, 17c, 17e.

The Cl-, the F-, and the OMe-derivatives (17b, 17c, 17e) all behaved as competitive inhibitors; showing no effect on apparent $k_{cat}$, while significantly increased the apparent $K_M$ value. The measured $K_i$ values for these compounds are shown in Table 1. The Dixon plot for 17c is shown in Figure 3B and in the supporting information for compounds 17c (Figure S6) and 17e (Figure S7).

Tryptophan fluorescence titration:

To validate the $K_I$ values from the NADH coupled assay, $K_D$ values were obtained from tryptophan fluorescence as a function of inhibitor concentration for each of the synthesized compounds (17b, 17c, 17e). The fluorescence changes due to the binding of 17b are shown in Figure 3b. The $K_D$ values for each of the compounds were measured in duplicate and are given in Table 1. The measured $K_D$ values are similar to the measured $K_i$ values.

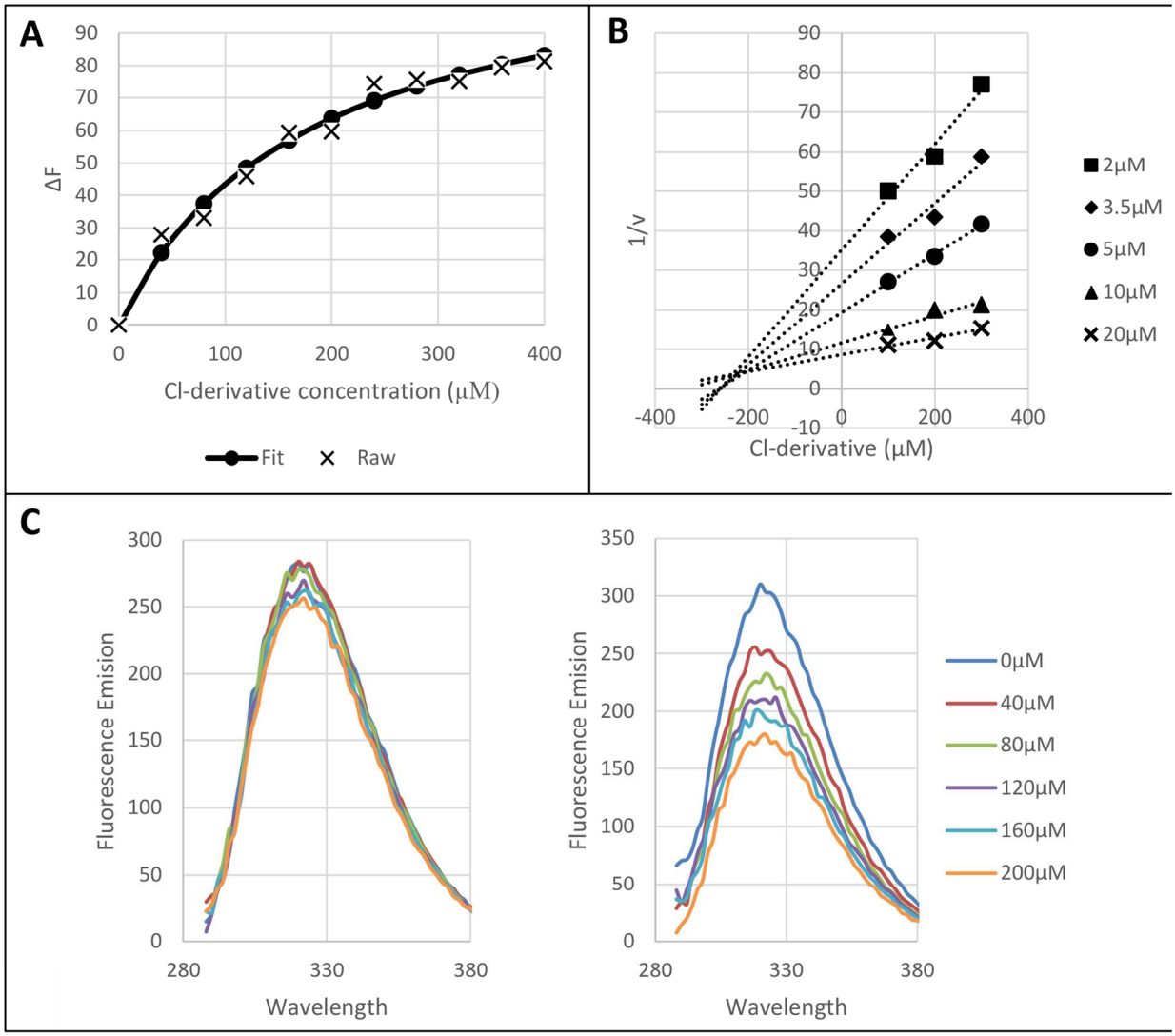


**Figure 3. Characterization of Cl-derivative (17b).** Panel A: $K_D$ estimation: ΔF is plotted against the concentration of the synthesized compound and fitted to a hyperbolic curve for the estimation of the $K_D$ value. The $K_D$ of compound 17b is estimated to be 175.08±1.56 μM. Panel B: Dixon plot for the estimation of $K_i$: 1/v is plotted against the concentration of the synthesized compound; the x-coordinate of the intercept of the trend lines = $-K_i$. The $K_i$ for compound 17b is estimated to be ~225 μM. Panel C: Left: Tryptophan fluorescence titration curve for F74A mutant. Right: Tryptophan fluorescence titration curve for Wild-type PfTMK.

Docking Simulation:

On the basis of docking simulations, the synthesized compounds share the same binding pocket with TMP and exhibit similar binding mode (Figure 4, S8, S9). The Cl-, F-, and OMe-derivatives exhibited favorable and similar binding energies (Cl-derivative (17b): -9.3 Kcal/mol; F-derivative (17c): -9.3 Kcal/mol; OMe-derivative (17e): -9.1 Kcal/mol), this suggests that substituting the functional groups on the terminal benzyl group has relatively small effect on the binding, as indicated by our $K_D$ measurements presented in table 1. The three compounds fit into the TMP binding pocket and retain the base stacking between the pyrimidine base and that of the aromatic ring of Phe74 residue, which is consistent with their activity as competitive inhibitors. The docking simulations also show that the alpha configuration facilitates interactions with His71 and Arg78 residues, which improves the interaction of the 3'OH with Tyr107 and Arg99. In addition to these residues, the docking simulation revealed that Asp17, Arg18, Lys21, Arg47, and Glu151 potentially interact with the synthesized compounds (see Figure 3 and Table 2).

The thymidine ring of the inhibitors stacks on the phenyl group of Phe74, in a similar manner to the substrate (TMP). The critical role of Phe74 in binding thymidine is shown by the fact that the F74A mutant has no enzymatic activity[28]. Consequently, the replacement of Phe74 with Ala (F74A) should significantly reduce the binding of the inhibitors to PfTMK.

The structural integrity of the F74A mutant was previously investigated using circular dichroism[28]. Those experiments indicated that there were no significant changes in the overall secondary structure of the F74A protein. To characterize the effect of this mutation on the tertiary structure of PfTMK, we compared 2D proton-carbon HSQC spectra of ILV labeled F74A protein to the ILV spectrum of wild-type protein (Figure. 4). A small number of methyl peak shifts were observed in the isoleucine region (presumably I55, and I70, as they are 4.7 Å and 5.9 Å away from Phe74), however the majority of the peaks were in similar positions.

Tryptophan fluorescence was used to determine the binding constant of the inhibitors to the F74A protein for the chlorine derivative (Figure 3C), as well as the fluoro (Figure S6C) and the methoxy derivative (Figure S7C). These data indicate that the affinity of the F74A protein for the inhibitors is considerably reduced, as would be expected due to loss of stacking between the

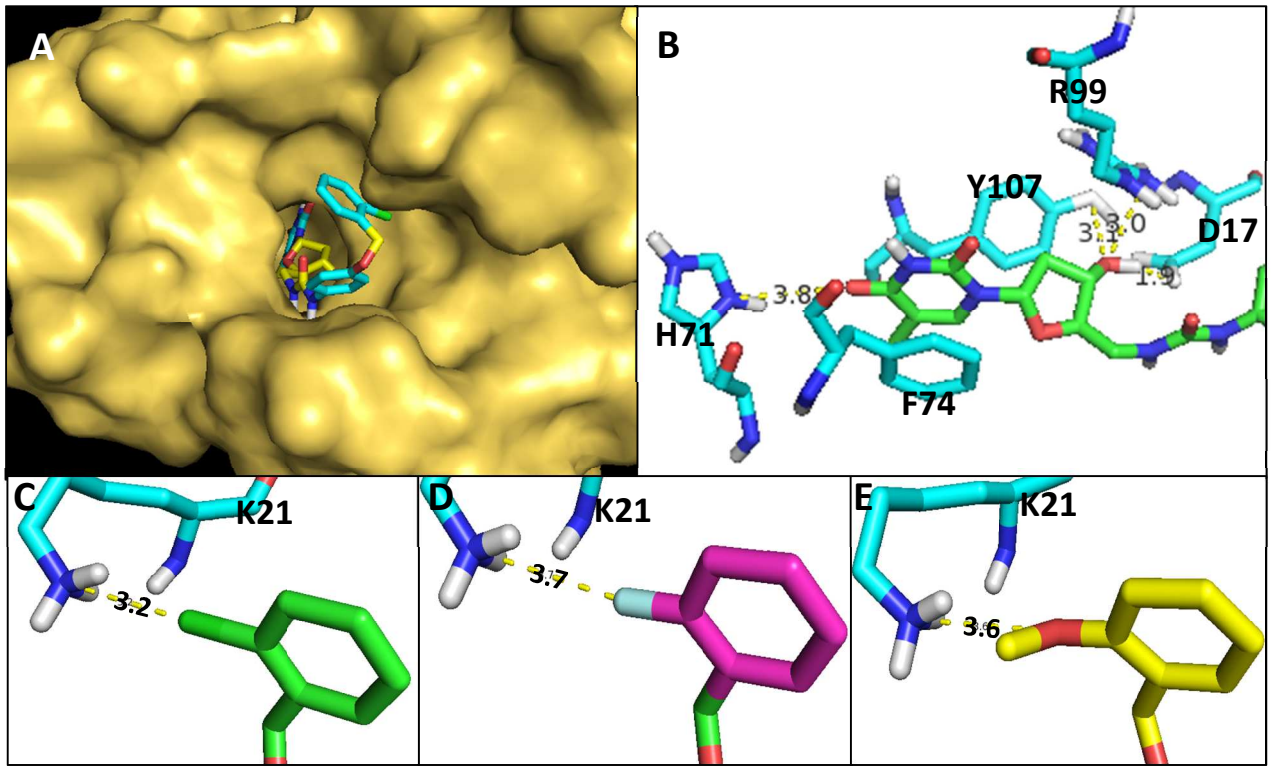


**Figure 4. Simulated Docking.** Panel A: Chloro-benzene substituent (17b) fits tightly into the TMP binding pocket with a binding energy of -9.3 Kcal/mol. Panel B: Atomic level detail of the α-thymidine moiety interacting with PfTMK. Panel C: Chloro-benzene substituent (compound 17b) interacting with Lys21. Panel D: Fluoro-benzene substituent (compound 17c) interacting with Lys21. Panel C: Methoxy-benzene substituent (compound 17e) interacting with Lys21.

thymidine base and F74.

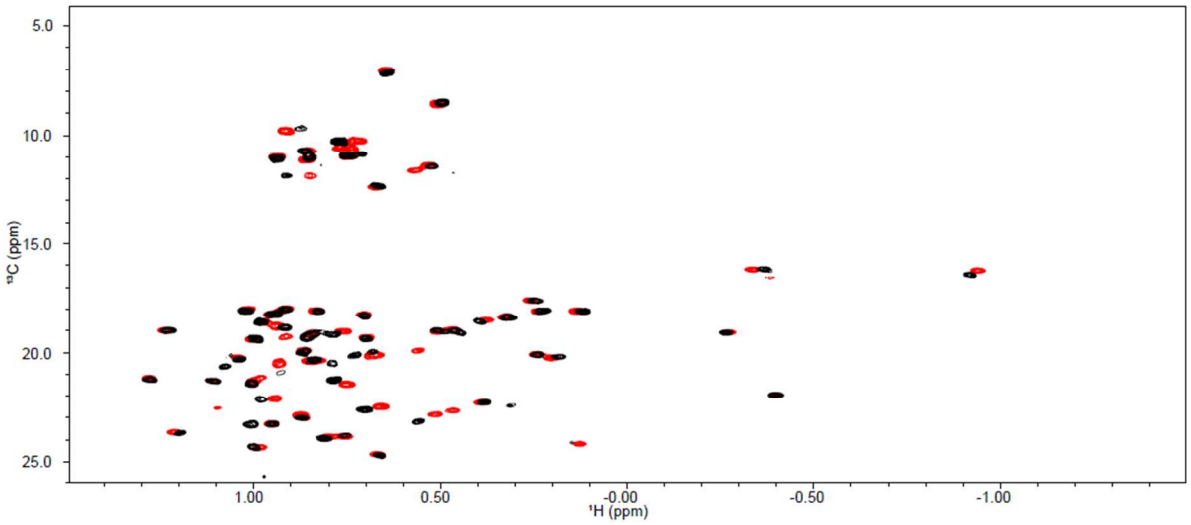


***Figure 5.*** **Overlay of PfTMK HMQC spectra of ILV methyls.** Wild-type PfTMK spectrum (black) is overlaid with the F74A mutant spectrum (red).

**Table 2**. Compound interaction with PfTMK

| Amino acid residue | Ligand |
|---|---|
| Tyr107 | 3'OH of TMP |
| Arg99 | 3'OH of TMP |
| Asp17 | 3'OH, urea linkage |
| Phe74 | Pyrimidine base |
| His71 | Pyrimidine base |
| Arg78 | Pyrimidine base |
| Glu151 | Urea linkage |
| Arg47 | Urea linkage |
| Arg18 | Phenol group |
| Lys21 | Terminal benzyl functional group |

## Conclusions

Here, we present strong evidence from enzyme inhibition, binding studies, docking simulation, and mutational studies that show that the Cl-, F-, and OMe-derivatives (17b, 17c, 17e) are all competitive inhibitors against PfTMK with comparable $K_i$ and $K_D$ values. Consequently, the chloro group can be substituted with electron withdrawing or donating groups (i.e. fluorine and methoxy) without significant changes in binding affinity.

Although the Cl-derivative (17b) is an efficient inhibitor of parasite growth, with an impressive EC50 value of 28 nM[8], our experimental data show that the binding to PfTMK is relative weak, with $K_i$ values around 200 μM. This suggests that the physiological target of the Cl-derivative is unlikely to be PfTMK, but some other enzyme in the cell. Alternative explanations are that the Cl-derivative may accumulate to high concentrations intra-cellularly. Conversely, the effective growth inhibition could also be explained by the fact that the metabolite of the Cl-derivative consists of an epoxide, which could lethal to the organism.

Although the results from the docking simulation suggest that modifications could be made to the terminal benzyl group or the urea linkage that would improve binding of these inhibitors, the relatively high $K_I$ values for these compounds suggest that significant structural modifications will be required to increase their binding affinity. It is unclear if these changes would provide sufficient improvement to the binding energy such that they would become effective at inhibiting PfTMK and consequently growth of the parasite. Moreover, considering that the inhibition of growth by the Cl-derivative is likely due to off-target effects, the Cl-derivative may not serve as an optimal scaffold to investigate structure activity relationships (SAR) for this group of compounds with respect to PfTMK. Rather, it will be necessary to identify the true intracellular target of these compounds before attempting more detailed SAR studies.

Lastly, the high quality of the methyl NMR spectrum of the PfTMK enzyme indicates that it will be possible to utilize chemical shift perturbation of methyl groups to screen fragment libraries to identify new synthetic routes to more effective PfTMK inhibitors.

**Conflicts of interest**

There are no conflicts to declare.

**Acknowledgements**

This research was supported by funding from the Mellon College of Science to GSR. We thank Roberto Gil and Virgil Simplacenu for support of the NMR instrumentation.

**Supporting Information**

Details on chemical synthesis schemes to generate compounds. One-dimensional proton NMR spectra of compounds 17a-17e, with assignments. Interaction of F-derivative (17c) and O-Met derivative (17e) with wild-type and mutant (F74A) PfTMK, characterized by tryptophan fluorescence and enzyme inhibition. Images of docked compounds for F- and O-Me derivatives.

**For Table of Contents Use Only**

Interaction of α-Thymidine Inhibitors with Thymidylate Kinase from *Plasmodium falciparum*.

Mengshen (David) Chen[a], Kaustubh Sinha[a], Gordon S. Rule[a], Danith H. Ly[b*]

[a] Department of Biological Sciences, Carnegie Mellon University, 4400 5th Ave, Pittsburgh PA.

[b] Department of Chemistry, Carnegie Mellon University, 4400 5th Ave, Pittsburgh PA.

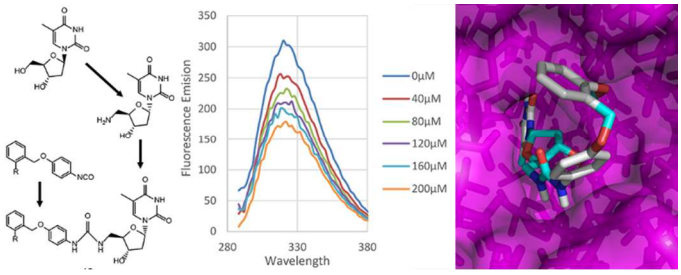

**References:**

[1] Ashley, E. a., Dhorda, M., Fairhurst, R. M., Amaratunga, C., Lim, P., Suon, S., Sreng, S., Anderson, J. M., Mao, S., Sam, B., Sopha, C., Chuor, C. M., Nguon, C., Sovannaroth, S., Pukrittayakamee, S., Jittamala, P., Chotivanich, K., Chutasmit, K., Suchatsoonthorn, C., Runcharoen, R., Hien, T. T., Thuy-Nhien, N. T., Thanh, N. V., Phu, N. H., Htut, Y., Han, K.-T., Aye, K. H., Mokuolu, O. a., Olaosebikan, R. R., Folaranmi, O. O., Mayxay, M., Khanthavong, M., Hongvanthong, B., Newton, P. N., Onyamboko, M. a., Fanello, C. I., Tshefu, A. K., Mishra, N., Valecha, N., Phyo, A. P., Nosten, F., Yi, P., Tripura, R., Borrmann, S., Bashraheil, M., Peshu, J., Faiz, M. A., Ghose, A., Hossain, M. A., Samad, R., Rahman, M. R., Hasan, M. M., Islam, A., Miotto, O., Amato, R., MacInnis, B., Stalker, J., Kwiatkowski, D. P., Bozdech, Z., Jeeyapant, A., Cheah, P. Y., Sakulthaew, T., Chalk, J., Intharabut, B., Silamut, K., Lee, S. J., Vihokhern, B., Kunasol, C., Imwong, M., Tarning, J., Taylor, W. J., Yeung, S., Woodrow, C. J., Flegg, J. a., Das, D., Smith, J., Venkatesan, M., Plowe, C. V., Stepniewska, K., Guerin, P. J., Dondorp, A. M., Day, N. P., and White, N. J. (2014) Spread of Artemisinin Resistance in Plasmodium falciparum Malaria, *New England Journal of Medicine 371*, 411-423.

[2] Bledsoe, G. H. (2005) Malaria primer for clinicians in the United States., *Southern medical journal 98*, 1197-1204; quiz 1205, 1230.

[3] Cassera, M. B., Zhang, Y., Hazleton, K. Z., and Schramm, V. L. (2011) Purine and pyrimidine pathways as targets in Plasmodium falciparum, *Current topics in medicinal chemistry 11*, 2103-2115.

[4] Ostermann, N., Schlichting, I., Brundiers, R., Konrad, M., Reinstein, J., Veit, T., Goody, R. S., and Lavie, A. (2000) Insights into the phosphoryltransfer mechanism of human thymidylate kinase gained from crystal structures of enzyme complexes along the reaction coordinate, *Structure 8*, 629-642.

[5] Lavie, A., Konrad, M., Brundiers, R., Goody, R. S., Schlichting, I., and Reinstein, J. (1998) Crystal structure of yeast thymidylate kinase complexed with the bisubstrate inhibitor P1-(5'-adenosyl) P5-(5'-thymidyl) pentaphosphate (TP5A) at 2.0 A resolution: Implications for catalysis and AZT activation, *Biochemistry 37*, 3677-3686.

[6] Fioravanti, E., Haouz, A., Ursby, T., Munier-Lehmann, H., Delarue, M., and Bourgeois, D. (2003) Mycobacterium tuberculosis thymidylate kinase: Structural studies of intermediates along the reaction pathway, *Journal of Molecular Biology 327*, 1077-1092.

[7] Caillat, C., Topalis, D., Agrofoglio, L. a., Pochet, S., Balzarini, J., Deville-Bonne, D., and Meyer, P. (2008) Crystal structure of poxvirus thymidylate kinase: an unexpected dimerization has implications for antiviral therapy., *Proceedings of the National Academy of Sciences of the United States of America 105*, 16900-16905.

[8] Cui, H., Carrero-Lerida, J., Silva, a. P., Whittingham, J. L., Brannigan, J. a., Ruiz-Perez, L. M., Read, K. D., Wilson, K. S., Gonzalez-Pacanowska, D., and Gilbert, I. H. (2012) Synthesis and evaluation of alpha-thymidine analogues as novel antimalarials, *Journal of medicinal chemistry 55*, 10948-10957.

[9] Sinha, K., and Rule, G. S. (2017) The Structure of Thymidylate Kinase from Candida albicans Reveals a Unique Structural Element, *Biochemistry 56*, 4360-4370.

[10] Whittingham, J. L., Carrero-Lerida, J., Brannigan, J. a., Ruiz-Perez, L. M., Silva, A. P. G., Fogg, M. J., Wilkinson, A. J., Gilbert, I. H., Wilson, K. S., and González-Pacanowska, D. (2010) Structural basis for the efficient phosphorylation of AZT-MP (3'-azido-3'-deoxythymidine monophosphate) and dGMP by Plasmodium falciparum type I thymidylate kinase., *The Biochemical journal 428*, 499-509.

[11] Martinez-Botella, G., Breen, J. N., Duffy, J. E., Dumas, J., Geng, B., Gowers, I. K., Green, O. M., Guler, S., Hentemann, M. F., Hernandez-Juan, F. A., Joseph-McCarthy, D., Kawatkar, S., Larsen, N. A., Lazari, O., Loch, J. T., Macritchie, J. A., McKenzie, A. R.,

Newman, J. V., Olivier, N. B., Otterson, L. G., Owens, A. P., Read, J., Sheppard, D. W., and Keating, T. A. (2012) Discovery of selective and potent inhibitors of gram-positive bacterial thymidylate kinase (TMK), *Journal of medicinal chemistry 55*, 10010-10021.

[12] Martinez-Botella, G., Loch, J. T., Green, O. M., Kawatkar, S. P., Olivier, N. B., Boriack-Sjodin, P. A., and Keating, T. A. (2013) Sulfonylpiperidines as novel, antibacterial inhibitors of Gram-positive thymidylate kinase (TMK), *Bioorganic & medicinal chemistry letters 23*, 169-173.

[13] Van Poecke, S., Munier-Lehmann, H., Helynck, O., Froeyen, M., and Van Calenbergh, S. (2011) Synthesis and inhibitory activity of thymidine analogues targeting Mycobacterium tuberculosis thymidine monophosphate kinase, *Bioorganic & medicinal chemistry 19*, 7603-7611.

[14] Familiar, O., Munier-Lehmann, H., Ainsa, J. A., Camarasa, M. J., and Perez-Perez, M. J. (2010) Design, synthesis and inhibitory activity against Mycobacterium tuberculosis thymidine monophosphate kinase of acyclic nucleoside analogues with a distal imidazoquinolinone, *European journal of medicinal chemistry 45*, 5910-5918.

[15] Choi, J. Y., Plummer, M. S., Starr, J., Desbonnet, C. R., Soutter, H., Chang, J., Miller, J. R., Dillman, K., Miller, A. A., and Roush, W. R. (2012) Structure guided development of novel thymidine mimetics targeting Pseudomonas aeruginosa thymidylate kinase: from hit to lead generation, *Journal of medicinal chemistry 55*, 852-870.

[16] Kato, A., Yasuda, Y., Kitamura, Y., Kandeel, M., and Kitade, Y. (2012) Carbocyclic thymidine derivatives efficiently inhibit Plasmodium falciparum thymidylate kinase (PfTMK), *Parasitology International 61*, 501-503.

[17] Noguchi, Y., Yasuda, Y., Tashiro, M., Kataoka, T., Kitamura, Y., Kandeel, M., and Kitade, Y. (2013) Synthesis of carbocyclic pyrimidine nucleosides and their inhibitory activities against Plasmodium falciparum thymidylate kinase, *Parasitology International 62*, 368-371.

[18] Jerina, D. M., and Daly, J. W. (1974) Arene oxides: a new aspect of drug metabolism, *Science (New York, N.Y.) 185*, 573-582.

[19] Burka, L. T., Plucinski, T. M., and Macdonald, T. L. (1983) Mechanisms of hydroxylation by cytochrome P-450: metabolism of monohalobenzenes by phenobarbital-induced microsomes, *Proceedings of the National Academy of Sciences of the United States of America 80*, 6680-6684.

[20] Sato, Y., Tateno, G., Seio, K., and Sekine, M. (2002) A convenient method for the conversion of beta-thymidine to alpha-thymidine based on TMSOTf-mediated C1 '-epimerization, *Tetrahedron Lett. 43*, 3251-3254.

[21] Ward, D. I., Jeffs, S. M., Coe, P. L., and Walker, R. T. (1993) A mild procedure for the anomerization of 2'-deoxynucleosides, *Tetrahedron Lett. 34*, 6779-6782.

[22] Bourne, E. J., Randles, J. E. B., Stavey, M., Tatlow, J. C., and Tedder, J. M. (1954) Studies of Trifluoroacetic Acid. Part X.1 The Mechanisms of Syntheses Effected by Solutions of Oxyacids in Trifluoroacetic Anhydride, *J. Am. Chem. Soc. 76*, 3206-3208.

[23] Studier, F. W., Rosenberg, A. H., Dunn, J. J., and Dubendorff, J. W. (1990) Use of T7 RNA polymerase to direct expression of cloned genes, *Methods in enzymology 185*, 60-89.

[24] Studier, F. W. (2005) Protein production by auto-induction in high-density shaking cultures, *Protein Expression and Purification 41*, 207-234.

[25] Goto, N. K., and Kay, L. E. (2000) New developments in isotope labeling strategies for protein solution NMR spectroscopy, *Curr. Opin. Struct. Biol. 10*, 585-592.

[26] Blondin, C., Serina, L., Wiesmuller, L., Gilles, A. M., and Barzu, O. (1994) Improved spectrophotometric assay of nucleoside monophosphate kinase activity using the pyruvate kinase/lactate dehydrogenase coupling system, *Analytical biochemistry 220*, 219-221.

[27] Hemsley, A., Arnheim, N., Toney, M. D., Cortopassi, G., and Galas, D. J. (1989) A simple method for site-directed mutagenesis using the polymerase chain reaction, *Nucleic acids research 17*, 6545-6551.
[28] Kandeel, M., Ando, T., Kitamura, Y., Abdel-Aziz, M., and Kitade, Y. (2009) Mutational, inhibitory and microcalorimetric analyses of Plasmodium falciparum TMP kinase. Implications for drug discovery., *Parasitology 136*, 11-25.
[29] Trott, O., and Olson, A. J. (2010) Software news and update AutoDock Vina: Improving the speed and accuracy of docking with a new scoring function, efficient optimization, and multithreading, *Journal of Computational Chemistry 31*, 455-461.
[30] (2015) Chemsketch version 14.01, Advanced Chemistry Development, Inc., Toronto, ON, Canada, www.acdlabs.com.
[31] Morris, G., and Huey, R. (2009) AutoDock4 and AutoDockTools4: Automated docking with selective receptor flexibility, *Journal of computational chemistry 30*, 2785-2791.
[32] *The PyMOL Molecular Graphics System, Version 1.8 Schrödinger, LLC.*
[33] Sato, Y., Tateno, G., Seio, K., and Sekine, M. (2002) Substituent and solvent effects of TMS triflate mediated C1' epimerization of b-thymidine to a-thymidine, *European Journal of Organic Chemistry*, 87-93.
[34] Kandeel, M., and Kitade, Y. (2008) Molecular characterization, heterologous expression and kinetic analysis of recombinant Plasmodium falciparum thymidylate kinase, *Journal of Biochemistry 144*, 245-250.

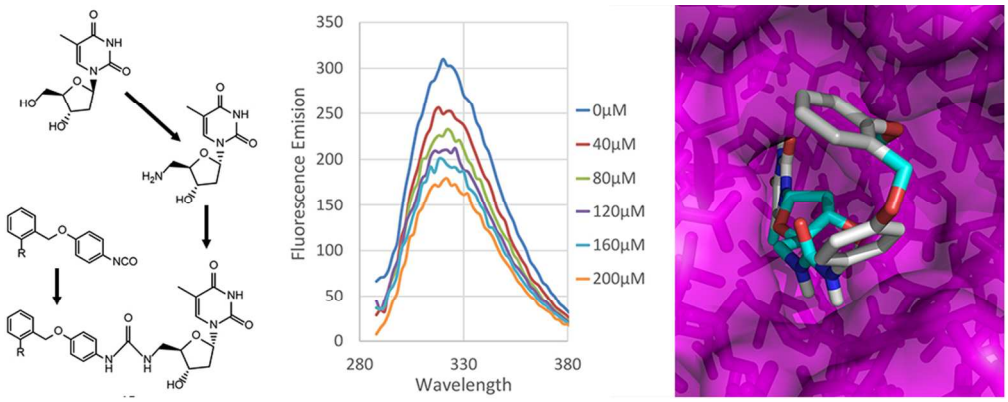


89x35mm (300 x 300 DPI)